Journal of Ultrafine Grained and Nanostructured Materials
https://jufgnsm.ut.ac.ir
Vol. 57, No.2, December 2024, pp. 177-189
Print ISSN: 2423-6845 Online ISSN: 2423-6837
DOI: 10.22059/jufgnsm.2024.02.08

PHEMA- PANI coating doped with silver nanoparticles for prevention of catheter-associated urinary tract biofilm infections

Behrooz Naghili[a], Raana Sarvari[a,b,c,1] , Elaheh Fakhri[d], Saleheh Abbaspoor[e], Mohammad Yousef Memar[a], Mehdi Sadrmohammadi[a]

[a]Infectious and Tropical Diseases Research Center, Tabriz University of Medical Sciences, Tabriz, Iran.
[b]Sarvaran Chemie Pishro Company (S.C.P), Tabriz, Iran
[c]Stem Cell Research Center, Tabriz University of Medical Sciences, Tabriz, Iran.
[d]Dental and Periodontal Research Center, Faculty of Dentistry, Tabriz University of Medical Sciences, Tabriz, Iran
[e]School of Engineering, Damghan University, Damghan, Iran.

Recieved: 5 October 2023; Accepted: 20 November 2024

[1]Corresponding author, E-mail: sarvarir@tbzmed.ac.ir

ABSTRACT

Long-term indwelling urinary catheters are associated with complications like infection and encrustation, which have brought patients burdens of health problems. Considering the damages caused by urinary tract infections, development of antibiofilm catheter coatings is a practical way to address this issue. Herein, we developed a PHEMA (poly(2- hydroxyethyl methacrylate))-PANI (polyaniline) based coating for stabilizing silver nanoparticles resulting in a high-performance antibiofilm catheter. For this purpose, silicone catheters were functionalized with OH groups and then 2- hydroxyethyl methacrylate (HEMA) was polymerized on the catheter by atom transfer radical polymerization (ATRP). The OH groups of PHEMA were converted into amine groups by reaction with para-anthranilic acid, and in the next step, PANI was produced by oxidation-reduction polymerization. In order to investigate the synergistic effects of silver nanoparticles on the antibacterial property of polyaniline, Ag nanoparticles were coated on polyaniline. Coated catheters were evaluated at each step using attenuated total reflection-fourier transform infrared (ATR-FTIR), scanning electron microscope (SEM), thermal gravimetric analysis (TGA), and atomic force microscopy (AFM). The water contact angle and consequently the hydrophilicity of the coated catheter have increased from 121˚ for the uncoated catheter to 101˚ for catheter-PHEMA-PANI and 73˚ for the catheter-PHEMA-PANI-Ag. Therefore, a hydrophilic PHEMA-PANI-Ag-coated catheter was developed with excellent thermal stability, antibacterial and antibiofilm properties against Escherichia coli and Pseudomonas aeruginosa during 24 and 48 hours and also improved biocompatibility on L929 fibroblast cells. It is concluded that the PHEMA-PANI-Ag-coated catheter with significant activity against antibiofilm formation is a potential candidate for indwelling urinary catheters and supports further clinical investigations.

Keywords: *Polyaniline; Hydrogel; Catheter; Nanoparticles; Antibiofilm; Coating.*

1. Introduction

Bacterial resistance is becoming a crucial threat to public health, and it is estimated that failure to address this problem will lead to 10 million deaths annually worldwide by 2050 [1-4]. Implantable devices are widely used to support or replace a part or whole of a biological structure in order to enhance a patient's quality of life but are also a major source of infection. Medical devices such as catheters and ventilators are susceptible to bacterial adhesion, reproduction, biofilm formation and as a result infection [5,6]. Medical device-related infections as the leading cause of secondary healthcare-associated bacteremia increase morbidity and mortality and impose a burden on the countries' health sector [5,7].

There are fundamental differences between bacteria in planktonic and multi-cellular or biofilm phases originating from the organized structure of biofilm [8]. In this mode, cells are in close proximity to each other and surrounded by a self-generated matrix containing exopolysaccharides, proteins, nucleic acids, and other bacterial debris [8, 9]. Furthermore, low metabolic activity along

with upregulation of genes required for anaerobic growth contribute to the long-lasting survival of biofilms explaining the increased biofilm tolerance to antibiotics, disinfectants and the immune system [8, 10-12].

Indwelling urinary catheters provide new bacteria adhesion sites and facilitate colonization of urinary pathogens. Following adherence of uropathogens including gram-negative (Pseudomonas aeruginosa, Escherichia coli and Klebsiella pneumonia) and gram-positive bacteria (Staphylococcus aureus) to catheter surface, secretion of extracellular mucopolysaccharide causes the formation of biofilm [13]. Biofilm structure reduces the sensitivity of colonizing bacteria to antibiotics and obstructs treatment modalities. Furthermore, uropathogens are capable of producing ureases that decompose urea into ammonia and providing an alkaline environment. Accumulation of insoluble hydroxyapatite and crystals of magnesium and calcium phosphate deposition as a result of increased pH accelerates the encrustation and obstructs the stent channel leading to far more complications including infection, bacteriuria, pyelonephritis and even septicemia [14, 15]. Catheter-related urinary tract infections can be dealt with by catheter replacement or antibiotic therapy inevitably resulting in the emergence of drug-resistant bacteria. Considering the higher economic and biological burden of long-term antibiotic therapy, consistent catheter care or complications of replacement surgery, designing and developing catheters with intrinsic antibacterial activity prove an attraction [16-19]. The existing anti-biofilm materials can be classified into the following categories: 1. Engineered surfaces with nano- or micro-topography preventing the adhesion of bacteria [20, 21], 2. Surfaces with stable antibacterial properties that destroy bacteria after adhesion [22] and 3. Surfaces with a slow release of antibiotics [23, 24]. All these features have been created using different functionalization approaches on the surfaces of medical devices including catheters [25].

In this regard, different compositions of coatings have been used to prevent biofilm formation including hydrogels [26], hydrophilic polymers [27], polytetrafluoroethanes [28], zwitterionic polymer coatings [29], and amphiphilic polymers [30, 31]. Moreover, coatings with antibacterial properties such as metal nanoparticles including silver, gold, copper, etc [32, 33], antibiotics [34], antimicrobial peptides [35], bacteriophages [36] and bioactive molecules [37] can be mentioned. Inorganic coatings including titanium, copper, silver and magnesium have been commonly applied on catheters for biofilm control. Prolonged activity has been obtained by the incorporation of nanoparticles into polymer substrates. According to the previous reports, immobilizing metal nanoparticles on polymer-pretreated silicone catheters obtained antibiofilm and antifouling properties [38-40].

Hydrogels are a group of insoluble and hydrophilic polymers consisting of a significant amount of water (up to 99%) when fully swollen, despite having solid-like characteristics that provide desirable properties such as increased mechanical strength [26]. Hydrogels present ideal and indispensable properties as coatings. Along with swelling, hydrogels generate a hydrophilic layer on the surface of the catheter, which prevents the absorption of proteins and formation of biofilm [25, 26]. Furthermore, hydrogels provide a high capacity to accommodate various antibacterial nanoparticles and biomolecules [31].

Wide applications of hydrogel coatings using different technologies have been applied in order to form a polymeric network with strong adhesion to various substrates. Hydrogel coatings are able to absorb water and expand in aquatic environments, as a result of which volume change causes severe stress in the hydrogel thin layer [41]. The physically coated hydrogel layers present a weak interaction with the substrates by non-covalent forces, so the coating can easily be detached from the surface. To improve the stability of hydrogel coatings and increase its adhesion to the substrate, it is necessary to connect the hydrogel to the substrate through stronger connections such as covalent bonds [42].

Conductive polymers include a series of materials that have conjugated double bonds in the polymer body, which facilitate electron movement and charge transfer between polymer chains and lead to high electrical conductivity [43]. Organic polymers that are widely studied are polyaniline [44], polypyrrole [45], polythiophene [46, 47] and vinylene polyphenylene [48]. Polyaniline is one of the conductive polymers with redox properties receiving much attention in the past decades [43]. Various recent studies have reported the antimicrobial activity of PANI [49] and PANI-coated surfaces against Pseudomonas aeruginosa, Escherichia coli and Staphylococcus aureus [50, 51].

Although studies reported various modifications of urinary catheter wall surface for reduction of bacteria viability and biofilm adherence and prevention of encrustation, research for development of durable antimicrobial catheters is still ongoing. In this regard, silicone catheters were functionalized with OH groups and then HEMA was polymerized on the catheter by ATRP, and in the next step, PANI was produced by oxidation-reduction polymerization. In order to investigate the synergistic effects of Ag nanoparticles on the antibacterial property of PANI, ultimately Ag nanoparticles were coated on polyaniline.

2. Experimental

2.1 Materials and Methods

The N,N-dicyclohexyl carbodiimide (DCC), 4-dimethylaminopyridine (DMAP), p-anthranilic acid were prepared from Sigma-Aldrich (USA) and used without any purification. The aniline monomer (Merck, Darmstadt, Germany) was distilled twice under the reduced pressure right before the application. Ammonium peroxydisulfate (APS, Merck) was purified through re-crystallization from ethanol at room temperature. HEMA (Merck) was dried over calcium hydride, and distilled under vacuum and then stored at −20 ˚C until used. Copper (I) chloride (CuCl) was obtained from Sigma-Aldrich and purified by stirring in acetic acid three times, then washed with ethanol and dried under vacuum. α- Bromoisobutyryl bromide (BIBB) and N, N, N′,N″,N″-pentamethyldiethylenetriamine (PMDETA) were purchased from Merck (Darmstadt, Germany). All other agents were also prepared from Merck and Sigma-Aldrich and purified according to the standard procedures.

2.2 Treatment of catheter with UV/Ozone

The ultraviolet/ozone (UV/O_3) treatment of the catheter surface was done in a UV/O_3 chamber (Jelight Company, Inc., Model 42-220, Irvine, CA, 253.7 nm radiation) to create hydroxyl groups. The catheter samples were put in the UV/O_3 chamber at a 20 mm distance from the UV lamp and radiated for 20 minutes.

2.3 HEMA polymerization on treated catheter surface (catheter-PHEMA)

Freshly (UV/O_3)-treated catheter samples were immersed in a solution of active initiators in dry tetrahydrofuran (THF) for 24 hours at room temperature under a nitrogen atmosphere [52]. The initiator-immobilized substrate was washed in ethanol to remove the physisorbed initiators and then dried under vacuum. HEMA monomer was polymerized on the initiator-immobilized catheter via ATRP polymerization by a reaction system containing HEMA/ligand/CuCl with a molar ratio of 100/2/1**.** The system was degassed and the polymerization proceeded for 48 hours at 65 ˚C. Then, the PHEMA-catheter was withdrawn from the reactor and washed in methanol to remove the residue monomer and physisorbed homopolymers from the surface and dried under vacuum.

2.4 Functionalization of PHEMA-catheter surface (catheter-PHEMA-NH_2)

Conversion of the OH groups of the PHEMA into the amine groups was achieved by reacting with para-anthranilic acid. The PHEMA-catheter samples were immersed in the solution containing para-anthranilic acid, DMAP, DCC, and 35 mL of THF and allowed the reaction to proceed under mixing overnight at room temperature to produce the aminated PHEMA chains on the catheter surface. The substrates were then rinsed with methanol to remove the adsorbed reagents and dried under vacuum.

2.5 Aniline polymerization on catheter-PHEMA-NH_2 (catheter-PHEMA-PANI)

A flask was charged with the catheter-PHEMA-NH_2, distilled water, aniline monomer, and H_2SO_4 (1M). The reaction mixture was stirred for 1 h, and the temperature was then reduced to 0 ˚C. In a separate container, APS was dissolved in deionized water, and it was subsequently added to the above-mentioned flask. The reaction mixture was stirred for 24 h at 0 ˚C, and subsequently, the reaction was terminated by pouring the contents of the flask into a large amount of methanol. The resultant product was washed several times with methanol and dried in vacuum [53].

2.6 Ag nanoparticles incorporation on catheter-PHEMA-PANI (catheter-PHEMA-PANI -Ag)

To prepare the catheter-PHEMA-PANI -Ag, catheter-PHEMA-PANI immersed in 50 mL of distilled water, and 4.0 ml of silver nitrate solution 0.012 $molL^{-1}$ was added, $NaBH_4$ was slowly added in a ratio of 6:1 to silver nitrate over 30 minutes. The reduction of Ag^+ was initiated immediately, as the solution changed from colorless to light yellow and ended up reddish. The nanostructure of the coating compounds is the highlight of the present design (Figure 1).

2.7 Antibacterial activity

Escherichia coli (ATCC 25922) and Pseudomonas aeruginosa (ATCC 27853) strains were subcultured on Mueller-Hinton agar plates (Merck, Darmstadt, Germany) and incubated at 37°C in anaerobic conditions for 24 hours for at 37°C. Single colonies were suspended in trypticase soy broth (TSB and 1% glucose) (Merck, Darmstadt, Germany) and incubated at 37°C for 24 hours and were diluted to a turbidity of 5×10^5 colony-forming unit [CFU]/ml using a spectrophotometer. Specimens were placed in a 24-well microplate, inoculated with 1 ml of bacterial suspension and incubated for 24 or 48 hours at 37°C. The inoculum was removed and the density of the microbial broth culture was determined by plating 10 µl of serially diluted inoculum on agar plates. To evaluate the antibiofilm activity, catheter samples were rinsed gently with the sterile phosphate-buffered solution for 1 minute to remove unattached cells and then placed in sterile tubes containing 1 ml of PBS and vortexed for 1 minute. The suspensions were

serially diluted, then 10 µl of each was suspended on Mueller-Hinton agar plates and incubated at 37°C and 5% CO_2 for 24 hours. After incubation, the colony-forming units (CFU/ml) were calculated [54].

2.8 Cell viability

L929 mouse fibroblast cell line was employed in the cytotoxicity test. The Dulbecco's Modified Eagle's Medium (Gibco; Thermo Fisher Scientific, Inc., Waltham, MA, USA) containing 10 % of fetal bovine serum (Gibco; Thermo Fisher Scientific, Inc., Waltham, MA, USA) and 100 U mL^{-1} Penicillin/Streptomycin (Gibco; Thermo Fisher Scientific, Inc., Waltham, MA, USA), was used as the culture medium. Briefly, sterilized coated and uncoated catheters were placed into 24-well plates and cells were seeded at a density of 10^5 cells/well and incubated at 37 °C with 5 % CO_2 for 24, 48 and 72 hours. After the incubation, the supernatant culture medium was removed and cells were washed with phosphate buffer saline 3 times. Next, 3-(4,5-dimethylthiazol-2-yl)-2,5-diphenyl tetrazolium bromide (MTT) solution was added and plates were incubated for 4 hours. Finally, the intracellular formazan crystals were dissolved by adding dimethyl sulfoxide (DMSO). The absorbance of the suspension was measured at 570 nm.

2.9. Characterization

ATR-FTIR spectra (Shimadzu, Japan) (400 cm^{-1} to 4000 cm^{-1}) of the samples were obtained at room temperature. Thermogravimetric analysis (TGA) was conducted under a nitrogen atmosphere in the temperature range of 25–700 °C at a heating rate of 10 °C min^{-1}. FESEM type 1430 VP (LEO Electron Microscopy Ltd, Cambridge, UK) was applied to characterize the surface morphology of samples. The wettability of the catheters was investigated via the drop water contact angle measurement using an OCA 20 plus contact angle meter system (Data Physics Instruments GmbH, Filderstadt, Germany). AFM (NanoSurf Core AFM, Nanosurf AG, Liestal, Switzerland) was applied for 3D exploration of the samples' surface.

3. Results and discussion

Among the most important health problems of the present century, we can mention hospital infections that impose heavy costs on the health and treatment system, prolonging the length of hospitalization and increasing the patients' death rate [7]. Permanent implanted medical devices are associated with various antibiotic-resistant hospital infections since the used materials are susceptible to bacterial adhesion, proliferation, biofilm formation and as a result, infection [5]. Considering the crucial

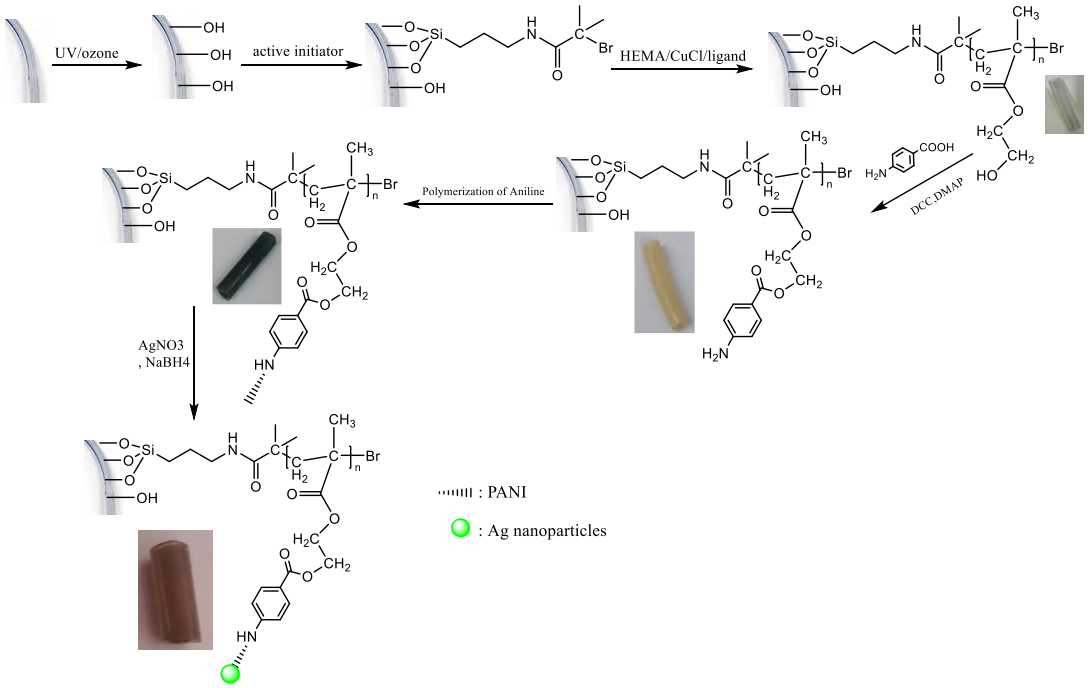

Fig. 1- Schematic illustration of the catheter coating.

threat of bacterial resistance to public health, in this project, we decided to design a coated catheter that both prevents biofilm formation and presents antibacterial properties resulting in limiting the need for antibiotic therapy in case of urinary tract infections. Modulating the nanostructure of the silicone catheter by coating PANI on the catheter surface and the Ag nanoparticle incorporation while maintaining the intrinsic properties including durability and stability were the aims of the present study. Since the morphology of the coated copolymer is brush-like, this feature is a factor in reducing biofilm formation due to the creation of spatial hindrance and subsequently preventing the adhesion of proteins related to bacteria.

3.1 ATR-FTIR

The ATR-FTIR spectra of catheter, catheter-PHEMA, catheter-PHEMA-PANI and catheter-PHEMA-PANI-Ag are shown in Figure 2. Catheter ATR-FTIR spectrum (Figure 2a) shows two stretching vibration bands at 1010 and 1077 cm^{-1} related to the Si-O-Si bond and a bending vibration band at 789 cm^{-1} attributed to the Si-OH bond [55-57]. The ATR-FTIR spectrum related to the catheter-PHEMA is presented in Figure 2b. The absorption bands observed in the catheter can also be seen in this spectrum. A slight difference can be seen only in the absorption intensity and wave numbers. In addition, the stretching vibration bands at about 3400-3500 cm^{-1} are related to OH groups of PHEMA. The rest of the bands corresponding to PHEMA overlaps with the previous bands. At the ATR-FTIR spectrum of catheter-PHEMA-PANI (Figure 2c), the observed band at 1258 cm^{-1} is related to the C-N absorption band and the bands observed at 300-3100 cm^{-1} are attributed to the vibrations of the aromatic C-H group and the bands observed at 1400-1600 cm^{-1} are related to the C=C stretching bands of the aromatic ring of polyaniline. At the ATR-FTIR spectrum of catheter-PHEMA-PANI-Ag (Figure 2d), the stretching vibration band at 3382 cm^{-1} is related to the NH_2 stretching bands of PANI and the stretching vibration band at 2963 cm^{-1} is related to the aliphatic C-H bonds and the stretching vibration bands at 1593 and 1507 cm^{-1} are related to the C=C stretching bands of the aromatic ring of polyaniline. ATR-FTIR spectrum confirms that amine groups of PANI have a strong binding affinity with silver nanoparticles.

3.2 Thermal stability

The TGA curves of catheter, catheter-PHEMA, and catheter-PHEMA-PANI are shown in Figure 3. According to Figure 3, all three samples have thermal stability up to 440 ˚C and all samples lost weight at higher temperatures, although the uncoated silicone sample has less weight loss at 700 ˚C and retained about 75% of its weight. Catheter-PHEMA (Figure 3) has a greater weight loss of 50% and kept only 50% of its weight at 700 ˚C. As expected, the catheter-PHEMA-PANI has a steeper weight loss at 700 ˚C and kept only 38% of its weight, which can be related to the degradation of PANI.

3.3 SEM

SEM images were used to evaluate the surface characteristics and changes in the morphology of the obtained products. Figure 4a is related to the image of the uncoated catheter. As can be seen in the figure, its surface is completely smooth without any kind of coatings. Figure 4b shows the SEM image of a PHEMA-coated catheter; surface is in the form of a sponge and has created an excellent coating on the catheter.

About catheter-PHEMA-PANI (Figure 4c) the catheter surface is in the form of wide plates, which confirms the polyaniline coating. Concerning the SEM image of catheter-PHEMA-PANI-Ag (Figure 4d and 4e) silver nanoparticles with a size of 29-30 nm are deposited on polyaniline plates. Furthermore, EDX results are shown in Figure 4 indicating the percentage of elements corresponding to the coating structure.

3.4 AFM

As can be seen in the AFM images in Figure 5, the surface morphology of uncoated catheters is significantly different from coated catheters at each stage. The uniform surface of the uncoated catheter in Figure 5a has become a surface with lumpy morphology, and with polymerization of HEMA (Figure 5b), an almost uniform surface but different from the uncoated catheter is created. The morphological changes observed in these images are completely consistent with the results obtained from the SEM images. According to the AFM, the PHEMA coating showed a non-flat surface and with the polymerization of PANI (Figure 5c), the morphology of the surface became somewhat smooth with regular grooves. In the case of catheter-PHEMA-PANI-Ag (Figure 5d), silver nanoparticles can be clearly seen in the form of spheres on the surface of PANI. Furthermore, the surface roughness values of the samples are listed in Table 1.

3.5 Wettability

Water contact angles are used as a qualitative sign of surface hydrophilicity. Images of the WCA analysis of catheter, catheter-PHEMA, catheter-PHEMA-PANI, and catheter-PHEMA-PANI-Ag are shown in Figure 6. As can be seen, with the continuation of the coating process, the WCA and consequently the hydrophilicity of the

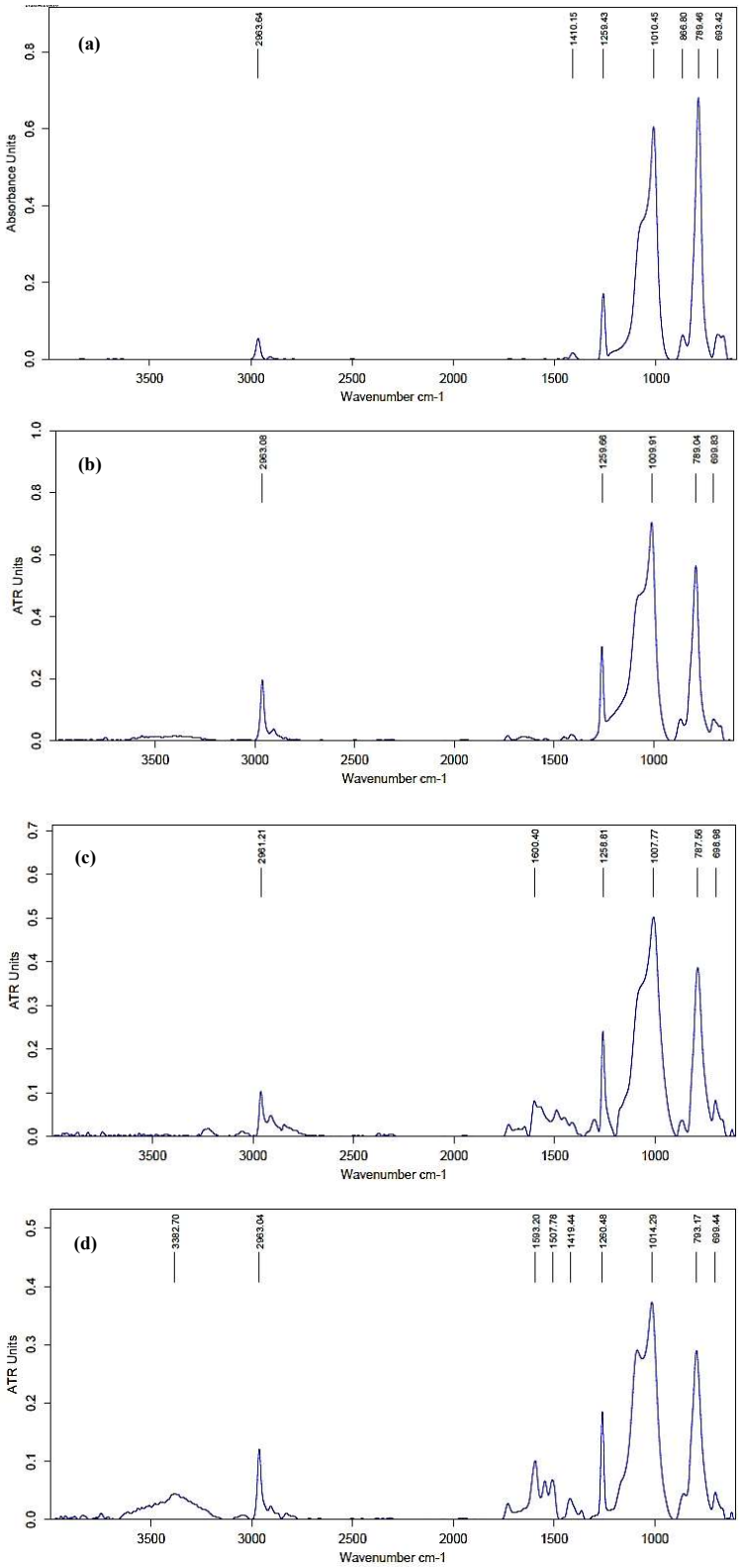

Fig. 2- ATR-FTIR spectrum of catheter (a), catheter-PHEMA (b), catheter-PHEMA-PANI (c), and catheter-PHEMA-PANI-Ag (d).

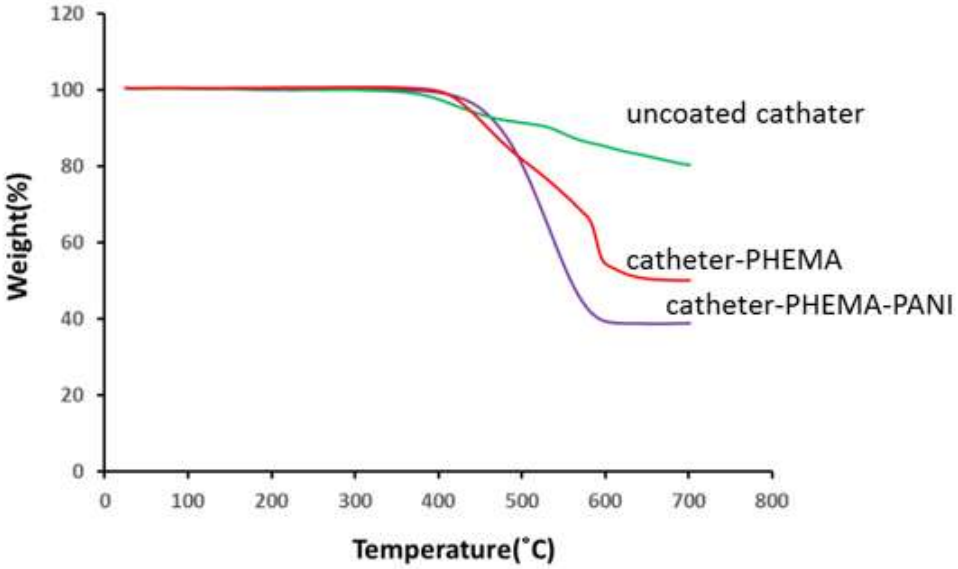

Fig. 3- TGA curves of catheter (green), catheter-PHEMA (red), and catheter-PHEMA-PANI (purple).

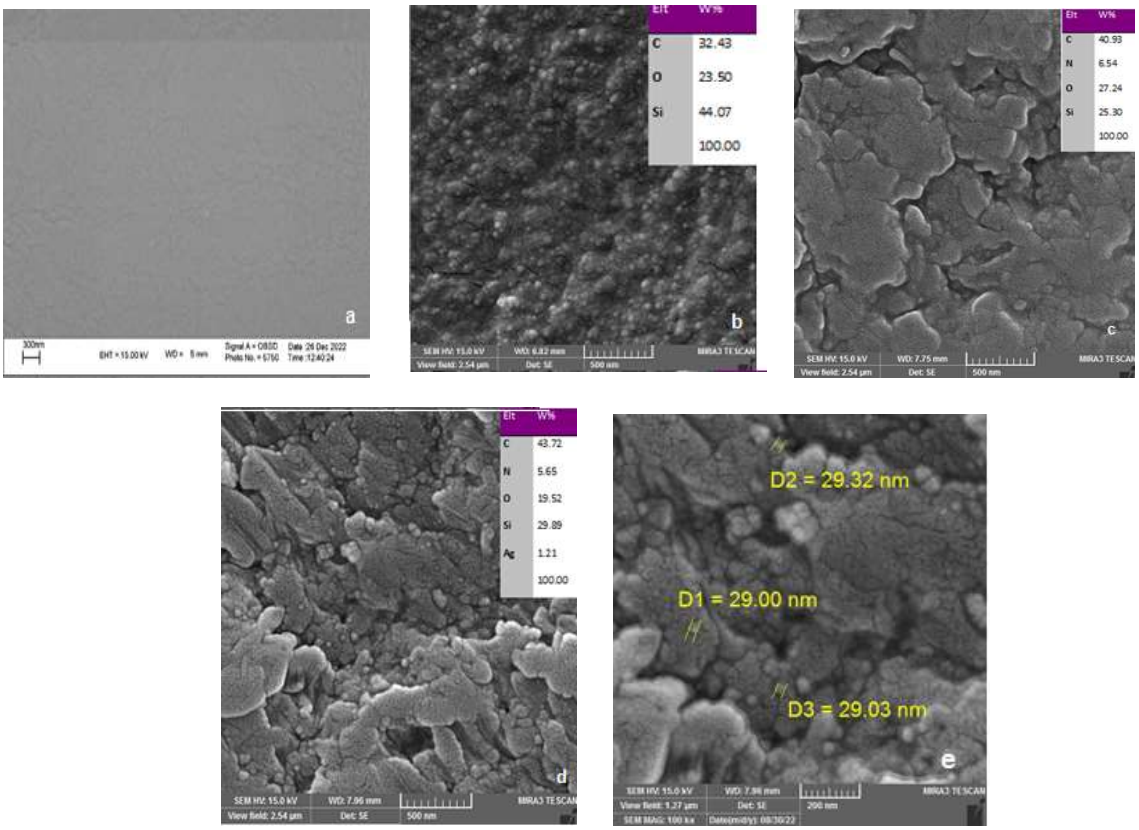

Fig. 4- SEM of catheter (a), and FESEM of catheter-PHEMA (b), catheter-PHEMA-PANI (c), and catheter-PHEMA-PANI-Ag (d and e).

coated catheter has increased from 116˚ for the uncoated catheter to 101˚ for catheter-PHEMA-PANI and 73˚ for the catheter-PHEMA-PANI-Ag. This indicates that PANI is more hydrophilic than silicone catheters. It has been established that structuring the catheter surface alters the surface wettability, affecting cell adhesion, proliferation and ultimately colonization [50].

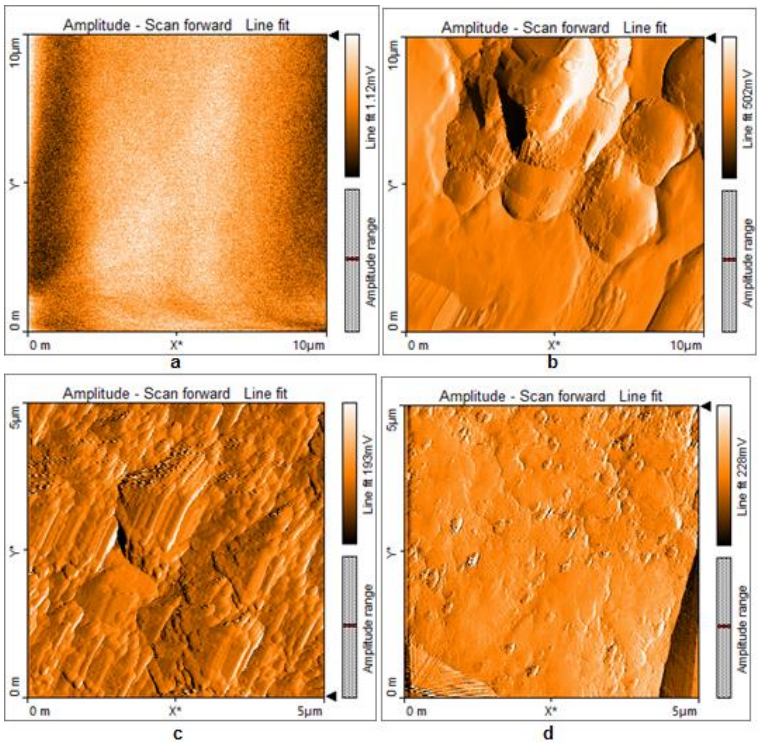

Fig. 5- AFM images of catheter (a), catheter-PHEMA (b), catheter-PHEMA-PANI (c), and catheter-PHEMA-PANI-Ag (d).

Table 1- The surface roughness values of the samples.

Sample	Surface Roughness (Ra)(nm)
catheter	10.80
catheter-PHEMA	117.98
catheter-PHEMA-PANI	167.41
catheter-PHEMA-PANI-Ag	33.39

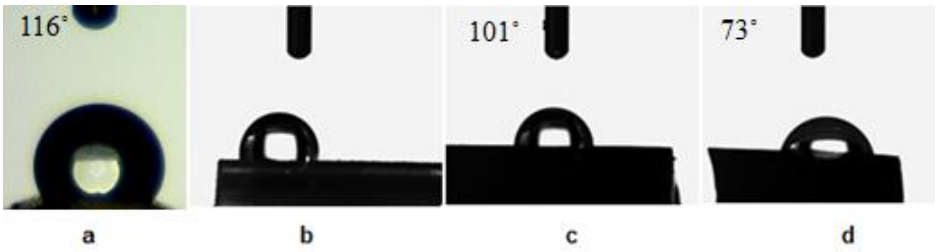

Fig. 6- Contact angle images of catheter (a), catheter-PHEMA (b), catheter-PHEMA-PANI (c), and catheter-PHEMA-PANI-Ag (d).

3.6 Antibacterial and antibiofilm properties

It is acknowledged that urinary tract infections are mainly caused by P. aeruginosa, E. coli, S. aureus and P. mirabilis. Ag nanoparticles inheriting a broad spectrum of antibacterial properties were applied in this study. Coated catheters at each stage were investigated for antibacterial activities against the bacterial growth in planktonic and biofilm states at 24 and 48 hours of bacterial incubation with the tested samples. In the present study, we focused on Gram-negative pathogens since no developed antibiotics have been approved for Gram-negative pathogens recently in spite of their growing threatening multidrug resistance [58, 59]. The antibacterial properties against P. aeruginosa and E. coli in planktonic and biofilm forms are shown in Figure 7. The uncoated sample did not demonstrate antibacterial activity in any bacterial growth states. Furthermore, the PHEMA-coated catheter showed no significant inhibition of planktonic or biofilm growth. The hydrophilic PANI-coated catheters showed no antibacterial effect for bacteria in the planktonic state. However, the highly hydrophilic nature of the surface impeded the bacteria adhesion and impaired the biofilm formation of both P. aeruginosa and E. coli during 24 and 48 hours, acting as an antifouling coating [60]. PANI-coated catheter achieved more than 2 log (CFU/ml) reduction of bacteria. PANI affects bacteria cell membrane and induces the expression of oxidative damage-responsive genes while repressing genes involved in metabolism, transport and cell wall synthesis [61]. These results corroborate the previous study regarding the inhibitory effects of PANI-coated surfaces against P. aeruginosa attachment and growth [50].

PHEMA-PANI-Ag-coated catheter inhibited the initial adherence of P. aeruginosa and E. coli and also exhibited an inhibitory effect against biofilm formation during 24 and 48 hours of incubation. Notwithstanding, the antibacterial effect of the Ag-coated samples did not differ by increasing time, obtaining an approximately 4 log(CFU/ml) and more than 99% reduction in viable bacteria. It can be concluded that bacterial adhesion was reduced on the PHEMA-PANI –coated catheters and strongly reduced on the PHEMA-PANI-Ag-coated catheter with excellent antibacterial and anti-adhesive activity against Gram-negative bacteria. Therefore, HEMA-PANI-Ag-coated catheter can be considered an advantageous catheter material compared to the commercially available silicone. The hydrophilic component of polymer-coated catheters that increased the hydrophilic balance along with the cationic characteristics of Ag nanoparticles decreased the bacterial viability. The cationic nature of Ag nanoparticles facilitates the adsorption to the bacterial membrane with negative charges and affects the integrity of the cell membrane by interfering with the membrane structure and permeability and consequently transport of various molecules through the membrane [60].

3.7 Cell Viability

Since nanoparticles at high concentrations inflict cytotoxicity on cells, the biocompatibility of the layered coating is considered an important factor to be assessed prior to clinical applications. Potential cytotoxic effects of coatings are shown in Figure 8. For this purpose, the L929 fibroblast cells were incubated on different coated catheters for 24, 48, and 72 hours and cell viability was assessed using the MTT method. The results showed that despite a slight decrease in cell proliferation on coated catheters during the first 24 hours, the final coated catheter (catheter-PHEMA-PANI-Ag) presented excellent cytocompatibility after 72 hours and the mean cell viability was over 93%, meaning the coated catheter is safe for further clinical applications. The cell repellency and antifouling properties of the coatings might be the main reason for low cell viability results.

4. Conclusions

In summary, a catheter coating based on polyaniline-hydrogel was designed and silver nanoparticles were incorporated into the polymeric substrate. The results revealed that PHEMA-PANI-Ag coating on the catheter surface presents a significant hydrophilicity compared to the uncoated one. The WCA and consequently the hydrophilicity of the coated catheter have improved from 121° for the uncoated catheter to 101° for catheter-PHEMA-PANI and 73° for the catheter-PHEMA-PANI-Ag. Therefore, a hydrophilic PHEMA-PANI-Ag-coated catheter was developed with excellent thermal stability, antibacterial and antibiofilm properties against Escherichia coli and Pseudomonas aeruginosa during 24 and 48 hours and also improved biocompatibility on L929 fibroblast cells. Furthermore, the PHEMA-PANI-coated catheter showed a significant antibiofilm formation activity against P. aeruginosa and E. coli, while the Ag-containing coated catheter exhibited strong antibacterial activity against both bacteria in both planktonic and biofilm states. It is concluded that the PHEMA-PANI-Ag-coated catheter is a potential solution for urinary catheter infections and supports further clinical investigations.

Competing interests

The authors declare that they have no conflict of interest.

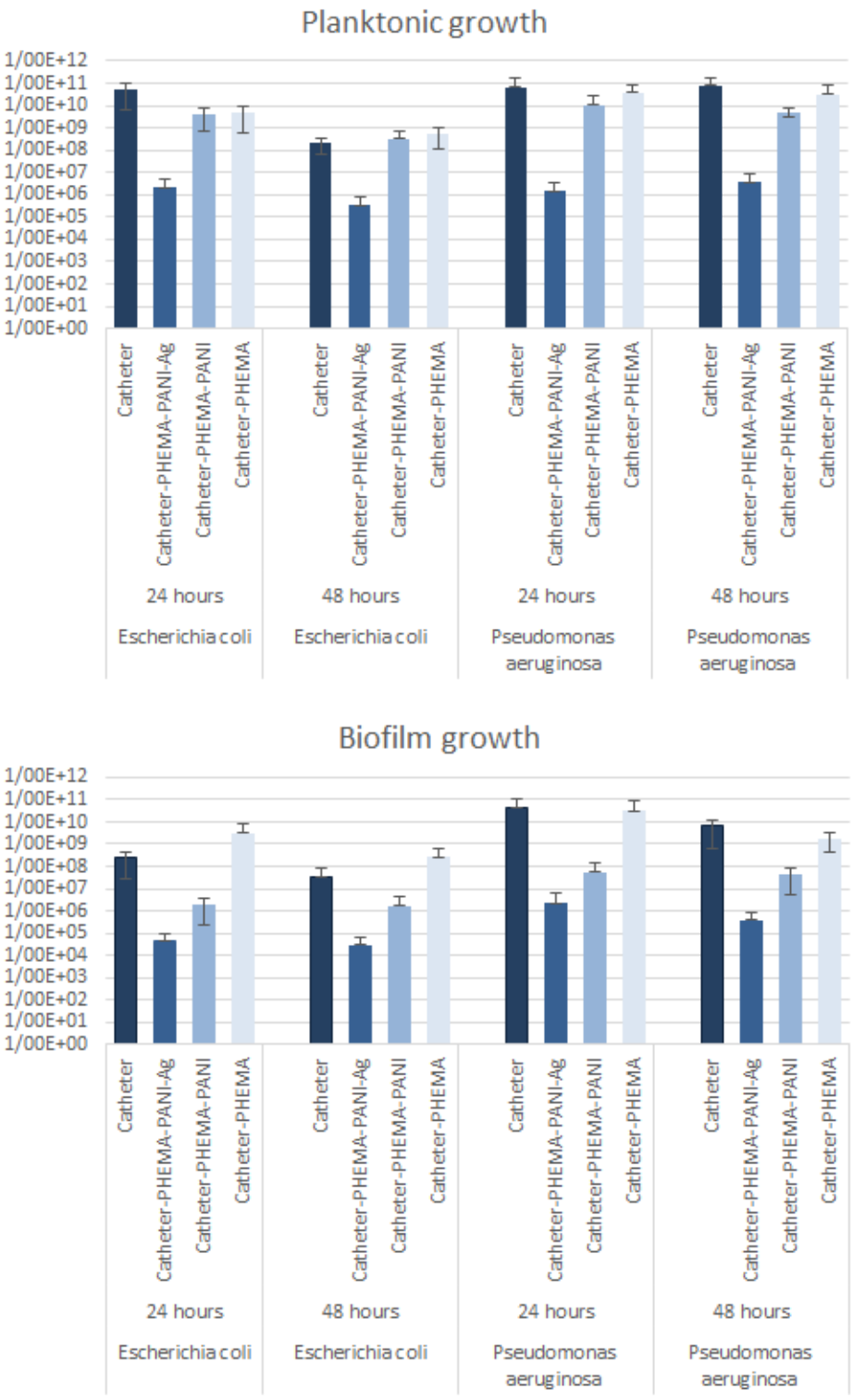

Fig. 7- The number of viable bacterial cells in CFU/ml for catheter (control), catheter-PHEMA, catheter-PHEMA-PANI, and catheter-PHEMA-PANI-Ag against P. aeruginosa and E. coli in planktonic and biofilm forms.

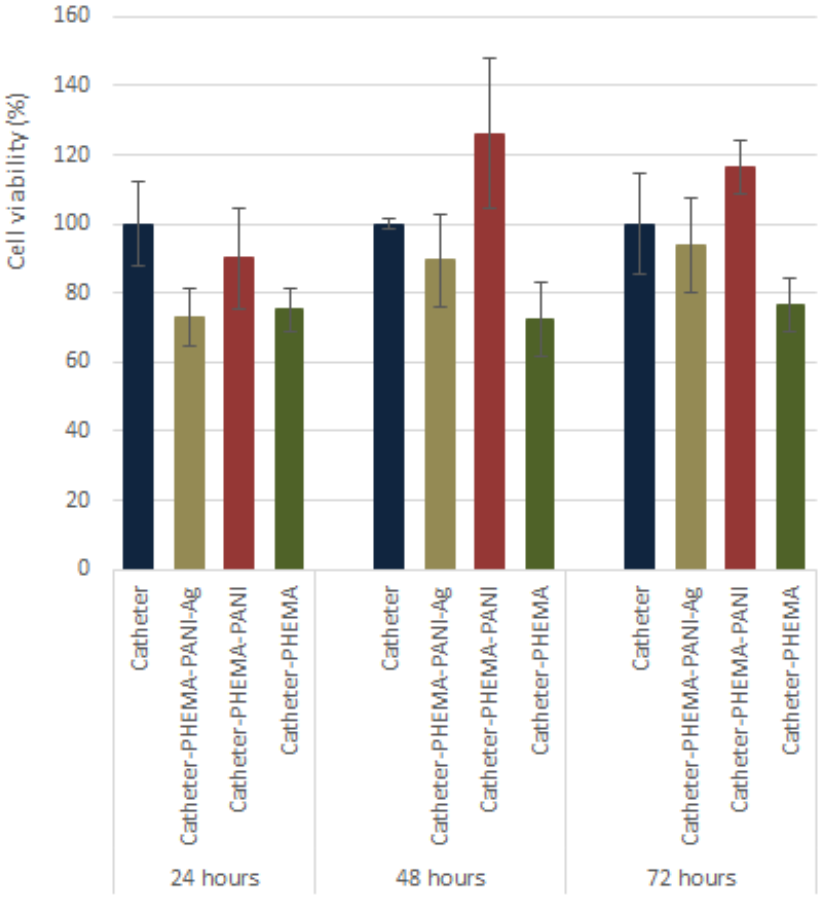

Fig. 8- Cytotoxic effects of catheter, catheter-PHEMA, catheter-PHEMA-PANI, and catheter-PHEMA-PANI-Ag on fibroblast cells.

Funding

This research has been supported by the Infectious and Tropical Diseases Research Center, Tabriz University of Medical Sciences, Tabriz, Iran (Grant Number: 67822).

References

1. Hassan M, Brede DA, Diep DB, Nes IF, Lotfipour F, Hojabri Z. Efficient inactivation of multi-antibiotics resistant nosocomial enterococci by purified hiracin bacteriocin. Advanced pharmaceutical bulletin. 2015;5(3):393.
2. Organization WH. Antimicrobial resistance: global report on surveillance: World Health Organization; 2014.
3. Shams F, Hasani A, Rezaee MA, Nahaie MR, Hasani A, Haghi MHSB, et al. Carriage of class 1 and 2 integrons in quinolone, extended-spectrum-β-lactamase-producing and multi drug resistant E. coli and K. pneumoniae: High burden of antibiotic resistance. Advanced pharmaceutical bulletin. 2015;5(3):335.
4. Sharifi Y, Hasani A, Ghotaslou R, Naghili B, Aghazadeh M, Milani M, et al. Virulence and antimicrobial resistance in enterococci isolated from urinary tract infections. Advanced pharmaceutical bulletin. 2013;3(1):197.
5. Percival SL, Suleman L, Vuotto C, Donelli G. Healthcare-associated infections, medical devices and biofilms: risk, tolerance and control. Journal of medical microbiology. 2015;64(4):323-34.
6. Weinstein RA, Darouiche RO. Device-associated infections: a macroproblem that starts with microadherence. Clinical infectious diseases. 2001;33(9):1567-72.
7. Dadi NCT, Radochová B, Vargová J, Bujdáková H. Impact of healthcare-associated infections connected to medical devices—an Update. Microorganisms. 2021;9(11):2332.
8. N. Hoiby, O. Ciofu, H.K. Johansen, Z.J. Song, C. Moser, P.O. Jensen, S. Molin, M. Givskov, T. Tolker-Nielsen, T. Bjarnsholt, The clinical impact of bacterial biofilms, Int. J. Oral Sci. 3 (2011) 55–65.
9. W. Hu, L. Li, S. Sharma, J. Wang, I. McHardy, R. Lux, Z. Yang, X. He, J.K. Gimzewski, Y. Li, W. Shi, DNA builds and strengthens the extracellular matrix in Myxococcus xanthus biofilms by interacting with exopolysaccharides, PLoS One 7 (2012) e51905.
10. B. Lee, C.K. Schjerling, N. Kirkby, N. Hoffmann, R. Borup, S. Molin, N. Hoiby, O. Ciofu, Mucoid Pseudomonas aeruginosa isolates maintain the biofilm formation capacity and the gene expression profiles during the chronic lung infection of CF patients, APMIS 119 (2011) 263–274.
11. P.O. Jensen, M. Givskov, T. Bjarnsholt, C. Moser, The immune system vs. Pseudomonas aeruginosa biofilms, FEMS Immunol. Med. Microbiol. 59 (2010) 292–305.
12. Hernández-Jiménez, Enrique, Rosa Del Campo, Victor Toledano, Maria Teresa Vallejo-Cremades, Aurora Muñoz,

Carlota Largo, Francisco Arnalich, Francisco García-Rio, Carolina Cubillos-Zapata, and Eduardo López-Collazo. "Biofilm vs. planktonic bacterial mode of growth: which do human macrophages prefer?." Biochemical and biophysical research communications 441, no. 4 (2013): 947-952.
13. Nicolle LE. Catheter associated urinary tract infections. Antimicrobial resistance and infection control. 2014;3:1-8.
14. Sabbuba N, Mahenthiralingam E, Stickler DJ. Molecular epidemiology of Proteus mirabilis infections of the catheterized urinary tract. Journal of clinical microbiology. 2003;41(11):4961-5.
15. Warren JW. Catheter-associated urinary tract infections. International journal of antimicrobial agents. 2001;17(4):299-303.
16. Sarvari R, Naghili B, Agbolaghi S, Abbaspoor S, Bannazadeh Baghi H, Poortahmasebi V, et al. Organic/polymeric antibiofilm coatings for surface modification of medical devices. International Journal of Polymeric Materials and Polymeric Biomaterials. 2022:1-42.
17. Khalil-Allafi J, Daneshvar H, Safavi MS, Khalili V. A survey on crystallization kinetic behavior of direct current magnetron sputter deposited NiTi thin films. Physica B: Condensed Matter. 2021 Aug 15;615:413086.
18. Mozetič M. Surface modification to improve properties of materials. Materials. 2019 Jan 31;12(3):441.
19. Safavi MS, Khalil-Allafi J, Ahadzadeh I, Walsh FC, Visai L. Improved corrosion protection of a NiTi implant by an electrodeposited HAp-Nb2O5 composite layer. Surface and Coatings Technology. 2023 Oct 15;470:129822.
20. Fadeeva E, Truong VK, Stiesch M, Chichkov BN, Crawford RJ, Wang J, et al. Bacterial retention on superhydrophobic titanium surfaces fabricated by femtosecond laser ablation. Langmuir. 2011;27(6):3012-9.
21. Dong Y, Li X, Bell T, Sammons R, Dong H. Surface microstructure and antibacterial property of an active-screen plasma alloyed austenitic stainless steel surface with Cu and N. Biomedical Materials. 2010;5(5):054105.
22. Hickok NJ, Shapiro IM. Immobilized antibiotics to prevent orthopaedic implant infections. Advanced drug delivery reviews. 2012;64(12):1165-76.
23. Wang X, Venkatraman SS, Boey FY, Loo JS, Tan LP. Controlled release of sirolimus from a multilayered PLGA stent matrix. Biomaterials. 2006;27(32):5588-95.
24. Xu Q, Czernuszka JT. Controlled release of amoxicillin from hydroxyapatite-coated poly (lactic-co-glycolic acid) microspheres. Journal of Controlled Release. 2008;127(2):146-53.
25. Andersen MJ, Flores-Mireles AL. Urinary catheter coating modifications: the race against catheter-associated infections. Coatings. 2019;10(1):23.
26. Dai S, Gao Y, Duan L. Recent advances in hydrogel coatings for urinary catheters. Journal of Applied Polymer Science. 2023;140(14):e53701.
27. Yu K, Alzahrani A, Khoddami S, Ferreira D, Scotland KB, Cheng JT, et al. Self-Limiting Mussel Inspired Thin Antifouling Coating with Broad-Spectrum Resistance to Biofilm Formation to Prevent Catheter-Associated Infection in Mouse and Porcine Models. Advanced Healthcare Materials. 2021;10(6):2001573.
28. Wang L, Zhang S, Keatch R, Corner G, Nabi G, Murdoch S, et al. In-vitro antibacterial and anti-encrustation performance of silver-polytetrafluoroethylene nanocomposite coated urinary catheters. Journal of Hospital Infection. 2019;103(1):55-63.
29. Peng W, Liu P, Zhang X, Peng J, Gu Y, Dong X, et al. Multi-functional zwitterionic coating for silicone-based biomedical devices. Chemical Engineering Journal. 2020;398:125663.
30. Stirpe M, Brugnoli B, Donelli G, Francolini I, Vuotto C. Poloxamer 338 affects cell adhesion and biofilm formation in escherichia coli: Potential applications in the management of catheter-associated urinary tract infections. Pathogens. 2020;9(11):885.
31. McCoy CP, Irwin NJ, Donnelly L, Jones DS, Hardy JG, Carson L. Anti-adherent biomaterials for prevention of catheter biofouling. International journal of pharmaceutics. 2018;535(1-2):420-7.
32. Roe D, Karandikar B, Bonn-Savage N, Gibbins B, Roullet J-B. Antimicrobial surface functionalization of plastic catheters by silver nanoparticles. Journal of antimicrobial chemotherapy. 2008;61(4):869-76.
33. Ballo MK, Rtimi S, Pulgarin C, Hopf N, Berthet A, Kiwi J, et al. In vitro and in vivo effectiveness of an innovative silver-copper nanoparticle coating of catheters to prevent methicillin-resistant Staphylococcus aureus infection. Antimicrobial agents and chemotherapy. 2016;60(9):5349-56.
34. Chatzinikolaou I, Finkel K, Hanna H, Boktour M, Foringer J, Ho T, et al. Antibiotic-coated hemodialysis catheters for the prevention of vascular catheter–related infections: a prospective, randomized study. The American journal of medicine. 2003;115(5):352-7.
35. Li X, Li P, Saravanan R, Basu A, Mishra B, Lim SH, et al. Antimicrobial functionalization of silicone surfaces with engineered short peptides having broad spectrum antimicrobial and salt-resistant properties. Acta biomaterialia. 2014;10(1):258-66.
36. Lehman SM, Donlan RM. Bacteriophage-mediated control of a two-species biofilm formed by microorganisms causing catheter-associated urinary tract infections in an in vitro urinary catheter model. Antimicrobial agents and chemotherapy. 2015;59(2):1127-37.
37. Nowatzki PJ, Koepsel RR, Stoodley P, Min K, Harper A, Murata H, et al. Salicylic acid-releasing polyurethane acrylate polymers as anti-biofilm urological catheter coatings. Acta Biomaterialia. 2012;8(5):1869-80.
38. Wang R, Neoh KG, Kang ET, Tambyah PA, Chiong E. Antifouling coating with controllable and sustained silver release for long-term inhibition of infection and encrustation in urinary catheters. Journal of Biomedical Materials Research Part B: Applied Biomaterials. 2015;103(3):519-28.
39. Gayani B, Dilhari A, Kottegoda N, Ratnaweera DR, Weerasekera MM. Reduced crystalline biofilm formation on superhydrophobic silicone urinary catheter materials. ACS omega. 2021;6(17):11488-96.
40. Gu G, Erişen DE, Yang K, Zhang B, Shen M, Zou J, et al. Antibacterial and anti-inflammatory activities of chitosan/copper complex coating on medical catheters: In vitro and in vivo. Journal of Biomedical Materials Research Part B: Applied Biomaterials. 2022;110(8):1899-910.
41 Wang, Shuyang, Zhengjin Wang, Yan Yang, and Tongqing Lu. "Swell induced stress in a hydrogel coating." Acta Mechanica Sinica 37, no. 5 (2021): 797-802.
42. Dai, Simin, Yang Gao, and Lijie Duan. "Recent advances in hydrogel coatings for urinary catheters." Journal of Applied Polymer Science 140, no. 14 (2023): e53701.
43. Namsheer K, Rout CS. Conducting polymers: A comprehensive review on recent advances in synthesis, properties and applications. RSC advances. 2021;11(10):5659-97.
44. Sarvari R, Agbolaghi S, Beygi-Khosrowshahi Y, Massoumi B. Towards skin tissue engineering using poly (2-hydroxy ethyl methacrylate)-co-poly (N-isopropylacrylamide)-co-poly (ε-caprolactone) hydrophilic terpolymers. International Journal of Polymeric Materials and Polymeric Biomaterials. 2019;68(12):691-700.
45. Hatamzadeh M, Sarvari R, Massoumi B, Agbolaghi S, Samadian F. Liver tissue engineering via hyperbranched polypyrrole scaffolds. International Journal of Polymeric Materials and Polymeric Biomaterials. 2020;69(17):1112-22.
46. Sarvari R, Massoumi B, Zareh A, Beygi-Khosrowshahi Y, Agbolaghi S. Porous conductive and biocompatible scaffolds on the basis of polycaprolactone and polythiophene for scaffolding. Polymer Bulletin. 2020;77:1829-46.
47. Agbolaghi S, Abbaspoor S, Massoumi B, Sarvari R, Sattari S, Aghapour S, et al. Conversion of Face-On Orientation to Edge-On/Flat-On in Induced-Crystallization of Poly (3-hexylthiophene) via Functionalization/Grafting of Reduced Graphene Oxide with Thiophene Adducts. Macromolecular Chemistry and Physics. 2018;219(4):1700484.
48. Zhang H, Zhong H, Dou F, Wang C, Wang S. Electrospinning

bifunctional polyphenylene-vinylene/heated graphene oxide composite nanofibers with luminescent-electrical performance. Thin Solid Films. 2021;725:138636.
49. Shi N, Guo X, Jing H, Gong J, Sun C, Yang K. Antibacterial effect of the conducting polyaniline. 2006.
50. Gallarato LA, Mulko LE, Dardanelli MS, Barbero CA, Acevedo DF, Yslas EI. Synergistic effect of polyaniline coverage and surface microstructure on the inhibition of Pseudomonas aeruginosa biofilm formation. Colloids and Surfaces B: Biointerfaces. 2017;150:1-7.
51. Seshadri DT, Bhat NV. Use of polyaniline as an antimicrobial agent in textiles. 2005.
52. Keyhanvar N, Zarghami N, Seifalian A, Keyhanvar P, Sarvari R, Salehi R, et al. The Combined Thermoresponsive Cell-Imprinted Substrate, Induced Differentiation, and" KLC Sheet" Formation. Advanced Pharmaceutical Bulletin. 2022;12(2):356.
53. Sarvari R, Massoumi B, Jaymand M, Beygi-Khosrowshahi Y, Abdollahi M. Novel three-dimensional, conducting, biocompatible, porous, and elastic polyaniline-based scaffolds for regenerative therapies. RSC advances. 2016;6(23):19437-51.
54. Badica P, Batalu N, Burdusel M, Grigoroscuta M, Aldica G, Enculescu M, et al. Antibacterial composite coatings of MgB2 powders embedded in PVP matrix. Scientific reports. 2021;11(1):9591.
55. Akhlaghi-Ardekani, N., Mohebbi-Kalhori, D. and Karazhyan, R., 2021. Improving Antibacterial and Anti-biofilmic properties of urological catheters with Eucalyptus, Rosemary, Green tea and Ziziphora extracts by impregnation method.
56. Massoumi, B., Sarvari, R. and Fakhri, E., 2024. Polyzwitterion coating based on PDMAEMA-block-PAAc for catheters with antibiofilm activities. International Journal of Polymeric Materials and Polymeric Biomaterials, pp.1-8.
57. Massoumi, B., Sarvari, R., Fakhri, E. and Vojoudi Fakhrnezhad, M., 2024. Silicon surfaces coated with polydopamine and poly (2-hydroxyethyl methacrylate) for medical device applications. Polymer Bulletin, pp.1-15.
58. Lam SJ, O'Brien-Simpson NM, Pantarat N, Sulistio A, Wong EH, Chen Y-Y, et al. Combating multidrug-resistant Gram-negative bacteria with structurally nanoengineered antimicrobial peptide polymers. Nature microbiology. 2016;1(11):1-11.
59. Lewis K. Platforms for antibiotic discovery. Nature reviews Drug discovery. 2013;12(5):371-87.
60. Pham P, Oliver S, Wong EHH, Boyer C. Effect of hydrophilic groups on the bioactivity of antimicrobial polymers. Polymer Chemistry. 2021;12(39):5689-703.
61. Gizdavic-Nikolaidis MR, Bennett JR, Swift S, Easteal AJ, Ambrose M. Broad spectrum antimicrobial activity of functionalized polyanilines. Acta biomaterialia. 2011;7(12):4204-9.